Research Article

Ocular Oncology and Pathology

Ocul Oncol Pathol 2019;5:276–283
DOI: 10.1159/000492599

Received: April 11, 2018
Accepted after revision: July 31, 2018
Published online: October 15, 2018

Monte Carlo Simulation of the Treatment of Uveal Melanoma Using Measured Heterogeneous ^{106}Ru Plaques

Francisco J. Zaragoza[b] Marion Eichmann[c] Dirk Flühs[b] Andrea Wittig[d] Wolfgang Sauerwein[b] Lorenzo Brualla[a]

[a]West German Proton Therapy Centre Essen (WPE), Essen, Germany; [b]NCTeam, Strahlenklinik, Universitätsklinikum Essen, Essen, Germany; [c]Fakultät Physik, Technische Universität Dortmund, Dortmund, Germany; [d]Klinik für Strahlentherapie und Radioonkologie, Universitätsklinikum Jena, Jena, Germany

Keywords
Monte Carlo simulation · Brachytherapy · PENELOPE · Ruthenium · Eye plaques · Beta emitter · Treatment planning · Uveal melanoma

Abstract
Background/Aims: Ruthenium plaques are used for the treatment of ocular tumors. The aim of this work is the comparison between simulated absorbed dose distributions tallied in an anthropomorphic phantom, obtained from ideal homogeneous plaques, and real eye plaques in which the actual heterogeneous distribution of ^{106}Ru was measured. The placement of the plaques with respect to the tumor location was taken into consideration to optimize the effectiveness of the treatment. ***Methods:*** The generic CCA and CCB, and the specific CCA1364 and CCB1256 ^{106}Ru eye plaques were modeled with the Monte Carlo code PENELOPE. To compare the suitability of each treatment for an anterior, equatorial and posterior tumor location, cumulative dose-volume histograms for the tumors and structures at risk were calculated. ***Results:*** Eccentric placements of the plaques, taking into account the inhomogeneities of the emitter map, can substantially reduce the dose delivered to structures at risk while maintaining the prescribed dose at the tumor apex. ***Conclusions:*** The emitter map distribution of the plaque and the computerized tomography of the patient used in a Monte Carlo simulation allow an accurate determination of the plaque position with respect to the tumor with the potential to reduce the dose to sensitive structures.

Introduction

Brachytherapy with ^{106}Ru eye applicators is a standard technique used for the treatment of uveal melanomas, the most common primary intraocular tumor. Although the use of ^{106}Ru applicators on uveal melanomas has been clinically studied, there is still a lack of precise knowledge on how the absorbed dose distribution in the tumor volume and the surrounding structures at risk determines the clinical outcome [1–5]. Obviously, misplacement of the plaque can cause underdosing of the tumor and the inclusion of structures at risk into the high-dose volume,

E-Mail karger@karger.com
www.karger.com/oop

Priv.-Doz. Dr. Lorenzo Brualla
West German Proton Therapy Centre Essen (WPE)
Hufelandstrasse 55
DE–45122 Essen (Germany)
E-Mail lorenzo.brualla@uni-due.de

resulting in less than optimal tumor control probability and enhanced side effects.

The Monte Carlo method is considered the gold standard for computing absorbed dose distributions, especially for small radiation fields [6, 7], the type of fields involved in eye treatments. During the last two decades, Monte Carlo algorithms have been used in some investigations to simulate the radiation transport process produced from ^{106}Ru eye plaques and to determine the resulting dose distributions [8–19]. It is assumed that the emitter substance in the plaque is homogeneously distributed. Also, most of them approximate the anatomy of the eye to a homogeneous water sphere where the anatomical structure of the eye and its corresponding structures at risk are not accounted for. Although some of the most recent works [15, 16] take into consideration the structures at risk, they still assume that the radioactive emitter substance is homogeneously distributed. Finally, Zaragoza et al. [20] determined the dose over a water phantom using a fine-grain probability map emission of the emitter substance previously measured over a specific CCA (CCA1364) and a CCB (CCB1256) eye plaque.

It is also well known that different applicator types result in different dose distributions. However, the influence of the individual distribution of the activity at the surface of individual applicators of the same size has not been fully investigated up to now. In fact, each individual eye plaque presents a different distribution of the emitter substance, hence, leading to slightly different 3D absorbed dose distributions from one applicator to another. In this study, we investigate the potential clinical benefit of considering such differences. Thus, in order to accurately plan a specific treatment, the emitter distribution of the individual eye plaque is required.

Methods and Materials

Geometry of the Plaques

The eye plaques considered in this work are the CCA1364 and the CCB1256 from the manufacturer BEBIG (Eckert & Ziegler BEBIG, Berlin, Germany). Both models are shaped as spherical caps obtained from a sphere of radius of 12.0 mm. The geometric difference between the plaques is the outer diameter of the shell across the rim, i.e., 15.5 mm for the CCA model and 20.2 mm for the CCB model. The plaques' structure, which is 1.0 mm thick in total, is divided into 3 layers. The thickness of each layer, from the inner to the outer surface, is 0.1, 0.2, and 0.7 mm. The layers are made of silver, with the middle layer containing the radioactive material, which is electrolytically deposited over its inner surface. The middle (active) layer is encapsulated between the inner (window) and the outer (shielding) layers and does not cover the whole cap, but it reaches up to 0.7 mm from the shell rim. For both plaques, the distribution of the emitter substance has been measured at the Technical University of Dortmund with a device specifically developed for this purpose [21]. The geometrical descriptions of the plaques [22] were accurately modeled using the constructive quadric geometry package provided with the general-purpose Monte Carlo radiation transport simulation code PENELOPE [23]. For comparison purposes, the idealized CCA and CCB plaques with a homogeneous emitter map were also simulated. The accuracy of our simulation system for eye plaques was previously validated by comparison of the simulated data in a water phantom with experimental results [10, 15]. The activities of the plaques used were those measured by the manufacturer and reported in the respective certificates, namely 11.6 MBq for the CCA1364 and 27.3 MBq for the CCB1256.

Simulation Codes

The radioactive isotope of ^{106}Ru disintegrates into ^{106}Rh producing a beta spectrum characterized by a maximum energy of 39 keV and a half-life of 368 days [24]. Then ^{106}Rh decays into stable ^{106}Pd producing a beta spectrum used for therapy. It is characterized by a maximum energy of 3.540 MeV and a half-life of 29.8 s.

Simulations were run with the PENELOPE (2008) code [23, 25] using penEasy (2010–09-07) [26] as the main steering program. penEasy was modified in two ways in order to simulate a beta decay spectrum and a heterogenous radiation source. To simulate the beta decay, an adapted version of the EFFY code [27], which uses the Fermi theory to describe the beta decay, was incorporated into the penEasy code. This modification allows to simulate the decay of ^{106}Rh into ^{106}Pd through the five disintegrations with the highest yields, i.e., 3.540 MeV (78.6%), 3.050 MeV (8.1%), 2.410 MeV (10.0%), 2.000 MeV (1.77%), and 1.539 MeV (0.46%). The second modification allows penEasy to randomly sample a position and a flight direction for each primary particle sampled over the plaque surface according to the probability distributions derived from the experimental heterogeneous emitter maps.

Voxelized Geometry

The fact that an emmetropic eyeball does not vary from one individual to another [28] allows to select a computerized tomography scan of an anonymized adult patient as an anthropomorphic voxelized phantom. This phantom has been used in previous works [16, 29, 30]. The computerized tomography scan has 256 × 256 × 59 voxels of 0.03125 × 0.03125 × 0.1 cm^3 size. Using the calibration curve of the computerized tomography scanner, Hounsfield numbers were converted into mass density values and three materials were chosen: air, water, and bone. penEasy allows to overlap quadric surfaces, those ones used to model the plaque as a spherical cap, on a voxelized geometry that one employed to represent the patient. This feature is used to simulate the geometry of the eye plaque positioned inside the voxelized human phantom.

Tumors and Sclera Segmentation

The general criteria used to select an appropriate plaque type for treatment is the basal diameter of the tumor, which determines the plaque size. The apical height of the tumor determines the irradiation time and the suitability of ^{106}Ru. In this work, the criterion selected to model the tumors was to maintain the basal diameter of 10.0 mm constant and to vary the apical height due to the fact that the tumor height is the critical parameter in a treatment.

These tumor volumes were modeled using a general paraboloid truncated by a sphere which coincided with the inner sclera surface. For segmentation purposes, we consider as sclera the spherical cap volume limited by the surfaces that contain, in the inner side, the base of the tumor and, in the outer side, the inner surface of the plaque. This spherical cap contains the anatomical sclera, some episcleral soft tissue and a safety margin that varies from 0.5 to 1 mm, depending on the variations of the thickness of the anatomical sclera in the different regions around the ocular globe. The whole volume considered was modeled with a thickness of 1.7 mm.

Although quadric surfaces were used as boundary surfaces to define all the significant elements in the segmentation process (i.e., tumors, sclera, and structures at risk), all these structures are defined in the computerized tomography and, as a consequence, many voxels are crossed by the quadrics. To consider if a given voxel is part or not of a segmented structure, the position of the center of the voxel is used as the belonging criterion. As a result of the above, both the thickness of the sclera and the tumor volume are determined by the voxelized segmentation. Therefore, the scleral thickness is not constant as it varies from approximately 1.2 to 2.1 mm, depending on the number of voxels included between the two spherical surfaces that define it. This variation is in agreement with the default value of 1.5 mm used in the code EYEPLAN [31, 32]. For the same reason, the apical height of a tumor can vary up to 0.5 mm from the quoted value. Since the eye plaques are defined as spherical caps with quadric surfaces, they are not affected by the approximations inherent to voxelized geometries, thus their thickness is constant.

Tumor Positioning and Plaque Placement

Tumor positioning was selected according to the maximum eye diameter in the axial plane of the computerized tomography. This means that the tumor symmetry axis and the eye diameter are coplanar. The equatorial plane of the eye was determined 15° above the horizontal axis of the computerized tomography and this plane contains the center of the eye. Tumors were placed in 3 positions: (1) equatorial, tumor symmetry axis intersects the eye equator; (2) anterior, tumor symmetry axis is set 15° above the equator, which means 30° over the horizontal axis, and (3) posterior, tumor symmetry axis is set 45° below the equator, that is, 60° below the horizontal axis. For all tumors, the apical height is considered from the tumor base. Equatorial tumors were modeled with the following apical heights: 3, 5, 6.5, 7, and 7.5 mm. Anterior and posterior tumors were modeled with an apical height of 3 mm. The distance from the posterior margin of the anterior and equatorial tumors to the papilla was 9.5 and 6.8 mm, respectively. The posterior margin of the posterior tumor overlapped by 2.8 mm with the papilla.

For simulating the treatments of the considered tumor volumes, the plaques were placed in different positions. For the 3-mm apical height anterior tumor, the homogeneous CCA plaque and the specific heterogeneous CCA1364 plaque were placed centrically with respect to the tumor, that means, the symmetry axis of the plaque coincided with the symmetry axis of the tumor. The CCA1364 was also studied in an eccentric position, that is, the symmetry axis of the plaque did not coincide with the symmetry axis of the tumor. Instead, the edge of the plaque was made tangent to the basal edge of the tumor at a point. This placement disregards the commonly used safety margin of 2 mm between the plaque and the basal edge of the tumor. For the equatorial tumors, with apical heights ranging from 3 to 7.5 mm, the homogeneous CCA and CCB plaques, as well as the heterogeneous CCA1364 and CCB1256 plaques, were all placed in a centric position. For the posterior tumor of an apical height of 3 mm, the homogeneous CCA and the heterogeneous CCA1364 plaques were simulated in eccentric placement, that is, the edge of the plaques was made tangent to the basal edge of the tumor at a point. This placement is anatomically difficult to attain with this plaque model owing to the presence of the optic nerve. A second, more eccentric placement was simulated for the heterogeneous CCA1364 plaque, which respected the anatomical position of the optic nerve. In this more eccentric placement, the plaque fell short of covering the whole basal surface of the tumor by a maximum distance of 0.3 mm. The heterogeneous CCB1256 was only placed equatorially, although it was also used for the eccentric treatment of the anterior and posterior tumors. The equatorially placed CCB1256 plaque covered the whole anterior tumor and the edge of the plaque overlapped the basal edge of the tumor by at most 2.8 mm. Conversely, the equatorially placed CCB1256 plaque did not fully cover the whole posterior tumor, with its edge falling short of the basal edge of the tumor by at most 2.6 mm.

The orientation of the plaques, that is, rotations about their symmetry axes, was considered in order to study the influence of the heterogeneities of the emission map. The CCB1256 eye plaque has a well-defined hot spot [20]. Although the CCB1256 eye plaque was positioned only equatorially, it is necessary to determine the effect of the relative position of the hot spot with respect to the structures at risk on the dose distribution for the anterior and posterior target volumes. In order to simulate the dose distribution in the anterior and posterior tumors, the CCB1256 plaque was rotated to take advantage of the hot spot position, that means, the spot was oriented in each case towards the considered tumor. For the CCA1364 eye plaque, the distribution of the radioactive substance over the surface does not present a hot spot, but it is not symmetrically and homogeneously distributed [20]. In this case, and taking advantage of the deposition of the radioactive substance for the anterior and posterior placements, the CCA1364 eye plaque was placed eccentrically and rotated in the appropriate way to protect structures at risk, while maximizing the dose to the apex. Figures 1 and 2 show the eccentric placement of the CCA1364 eye plaque in an anterior and a posterior position, respectively, and tangent to the basal line of the tumor.

Dose Prescription

Delivery of the dose takes a certain period of time, which is reflected in the prescription method. Initially, the time required to reach 700 Gy at the sclera, determined at a point 2 mm away from the plaque along its symmetry axis, is computed using the data corresponding to the heterogeneous configuration of the plaques obtained from a previous work [20]. For the computations presented herein, the aforementioned measured activities were used. These irradiation times are 132.8 h for treatments performed using the CCA1364 plaque and 93.8 h for treatments using the CCB1256 plaque. If the computed irradiation time is long enough to deliver a dose greater than 100 Gy at the tumor apex, then the treatment is performed. If not, the time is extended until the dose delivered at the apex reaches 100 Gy. If the new time results in a dose to the sclera greater than 1,500 Gy, then a brachytherapy treatment with this plaque is not performed.

Fig. 1. Isodose lines corresponding to the CCA1364 eye plaque placed eccentrically in an anterior position with respect to an anterior tumor of an apical height of 3 mm without respecting the 2-mm safety margin at the base of the tumor. The tumor volume is shown with a blueish color wash. Numbers next to each isodose line indicate absolute dose in Gy.

Fig. 2. Isodose lines corresponding to the CCA1364 eye plaque placed eccentrically in a posterior position with respect to a posterior tumor of an apical height of 3 mm without respecting the 2-mm safety margin at the base of the tumor. The tumor volume is shown with a reddish color wash. Numbers next to each isodose line indicate absolute dose in Gy.

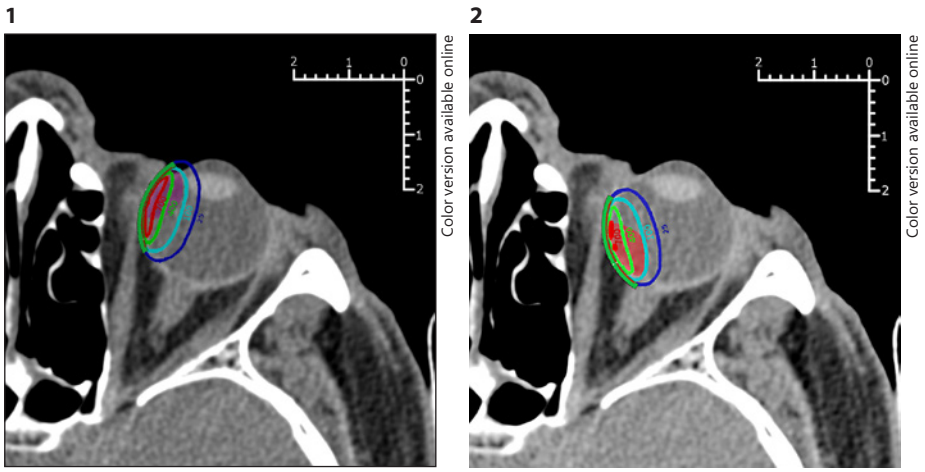

For this study, an apical dose of 100 Gy was chosen to improve comprehensibility. This value is not a recommendation for clinical applications. In clinical reality at the Universitätsklinikum Essen, the dose prescribed to the tumor apex is 130 Gy. This value takes into consideration the uncertainties associated with the treatment and leads to a clinical target volume that includes the gross tumor volume safely.

Results and Discussion

For all simulations performed, the average standard statistical uncertainty of the dose is lower than 1%.

In Figure 3, dose-volume histograms (DVHs) are plotted, obtained for the irradiations of an anterior 3-mm apical height tumor. The plot shows DVHs for the tumor volume and for the eye lens. The considered irradiations in that figure are the simulations performed with the generic homogeneous CCA plaque, the specific heterogeneous CCA1364 plaque placed centrically with respect to the tumor as well as eccentrically with respect to it, and finally, the specific heterogeneous CCB1256 eye plaque placed eccentrically, too. It is observed that the CCA1364 plaque placed centrically and the CCB1256 plaque placed eccentrically give similar coverage over the tumor volume. In terms of absolute dose, the maximum dose of 243 Gy at the tumor apex corresponds to the CCA1364 eye plaque, while the dose delivered by the CCB1256 plaque is 1.5% lower. The CCA1364 plaque placed eccentrically delivers at the tumor apex a maximum dose 23% lower than the dose delivered at the apex by the CCA1364 plaque placed centrically. With respect to the eye lens, the minimum dose of 91 Gy corresponds to the CCA1364 plaque placed eccentrically. The dose absorbed by the eye lens is 221% higher when using the CCA1364 eye plaque placed centrically and 155% when using the CCB1256 eye plaque.

Figure 4 represents the DVHs obtained for the cornea and the eye lens during the irradiation of a 3-mm apical height tumor in anterior position. The heterogeneous CCA1364 eye plaque placed centrically with respect to the tumor delivers the maximum dose to the cornea, that is, 44 Gy. This dose is 31% higher than the dose delivered by the heterogeneous CCB1256 and 49% higher than the dose delivered by the idealized homogeneous CCA eye plaque. The dose delivered to the cornea by the CCA1364 plaque placed eccentrically is lower than 1 Gy.

It was found that the treatment with the CCA1364 eye plaque placed eccentrically with respect to the 3-mm anterior tumor, without respecting the 2-mm safety margin, was the most suitable treatment, among those considered, in terms of the of the obtained DVHs. This configuration delivers the required dose at the tumor apex while minimizing the dose to the eye lens. It is also important to observe that the CCB1256 plaque placed eccentrically, on an equatorial position, delivers a smaller dose to the eye lens than the CCA1364 placed centrically.

Figure 5 shows the DVHs obtained for the tumor volume and the optic disc during the simulated irradiation of a tumor of 3 mm of apical height located in a posterior position of the eye. In terms of absolute dose, the CCA1364 eye plaque placed tangentially to the tumor delivers an apical dose of 158 Gy, which is the highest dose at the tumor apex among the simulated scenarios. The CCA1364

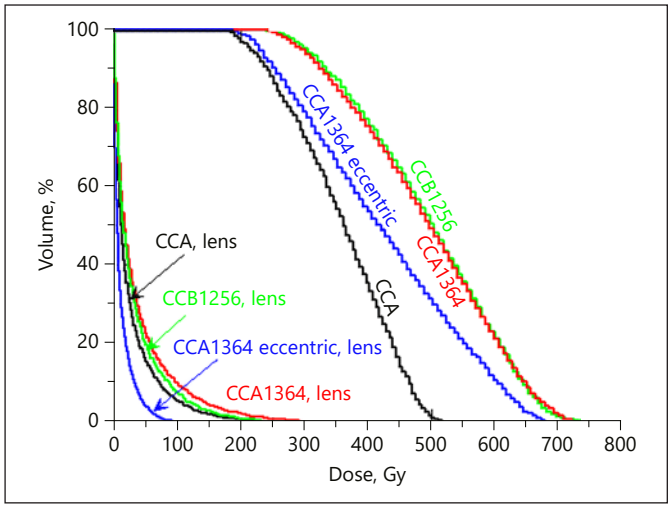

Fig. 3. Dose-volume histograms obtained for the eye lens and the anterior tumor volume of an apical height equal to 3 mm. The labels correspond to the following irradiations: "CCA" is a homogeneously distributed plaque placed centrically with respect to the tumor, "CCA1364" is the heterogeneously distributed plaque placed centrically, "CCA1364 eccentric" is the heterogeneous plaque placed eccentrically with the edge of the plaque made tangent to the basal edge of the tumor at a point, "CCB1256" is the heterogeneous plaque placed equatorially, that is eccentrically, and it covered the whole anterior tumor while the edge of the plaque overlapped the basal edge of the tumor by at most 2.8 mm. In all cases where heterogeneous plaques were used, they were oriented taking advantage of their heterogeneity to maximize the dose at the tumor volume and to minimize the dose at the structures at risk.

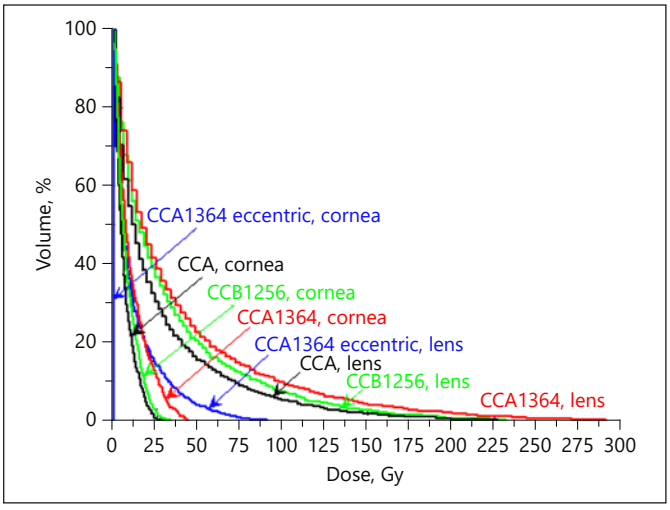

Fig. 4. Dose-volume histograms obtained for the cornea and the eye lens during the irradiation of a 3-mm apical height tumor in anterior position. The positions and orientations of the plaques indicated in the plots follow the same description given in the caption of Figure 3.

plaque delivers a 1.5% smaller dose when its position does not fully cover the base of the tumor. The homogeneous CCA plaque in the tangent position delivers a dose being 26% lower at the apex than the dose delivered by the CCA1364 in a tangent position. The CCB1256 plaque in the equatorial position delivers the lowest dose without reaching the reference dose of 100 Gy at the apex; this is 49% lower than the dose delivered by the CCA1364 placed tangentially to the tumor. Regarding the optic disc, the CCA1364 plaque placed tangentially to the tumor delivers a maximum dose of 956 Gy in its volume. When using the CCA1364 eye plaque without covering the whole base of the tumor, the maximum dose received by the optic disc is 13% lower than the dose delivered when the CCA1364 eye plaque is placed tangentially to the tumor base. The lowest dose to the optic disc is delivered by the CCB1256 plaque; this is 66% lower than the dose delivered by the CCA1364 plaque placed tangentially to the tumor.

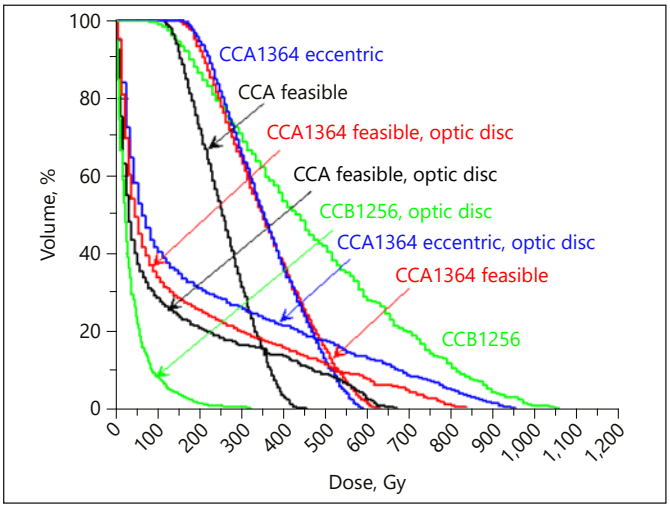

Fig. 5. Dose-volume histograms obtained for the tumor volume and the optic disc during the irradiation of a tumor of 3 mm of apical height located in a posterior position. The labels "CCA feasible" and "CCA1364 feasible" indicate an eccentric placement of the homogeneous and heterogeneous plaques, respectively, in which the whole base of the tumor is not covered owing to the presence of the optic nerve. In this placement, the plaque falls short by at most 0.3 mm to cover the base of the tumor. The label "CCA1364 eccentric" indicates an eccentric placement of the plaque in which the basal edge of the tumor is tangent to the edge of the plaque, a treatment which is not feasible due to the presence of the optic nerve. The label "CCB1256" indicates an equatorially located plaque that eccentrically treats the tumor. Its edge falls short by, at most, 2.6 mm to cover the base of the tumor.

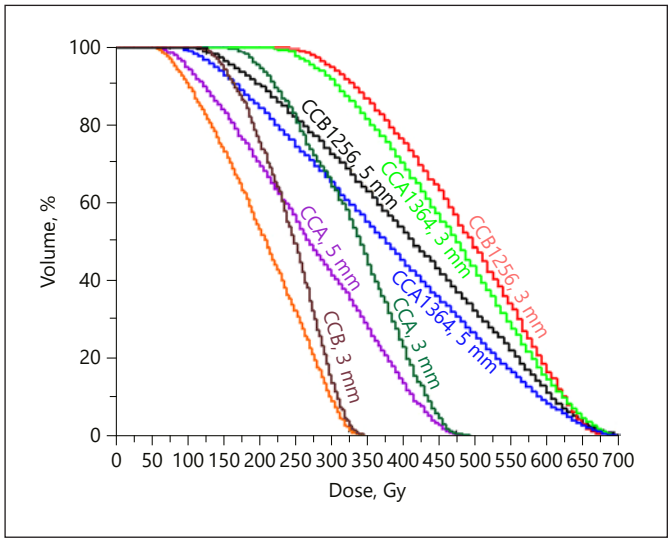

Fig. 6. Dose-volume histograms calculated for the tumor volume on tumors of 3 and 5 mm of apical height placed in an equatorial position. All plaques are centrically placed.

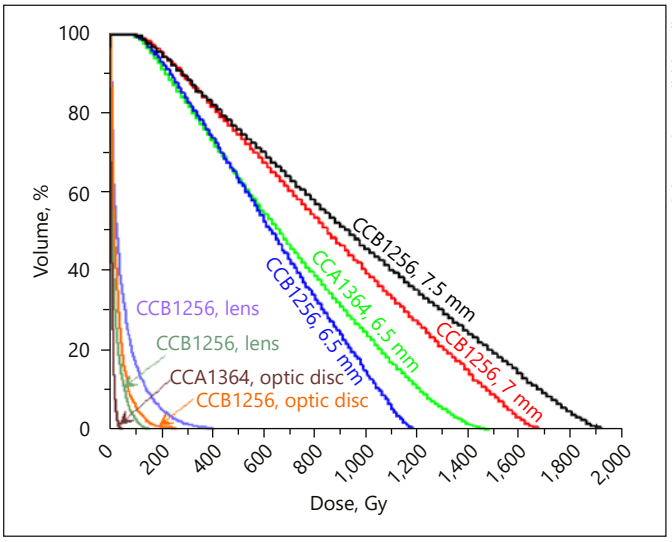

Fig. 7. Dose-volume histograms (DVHs) calculated for the tumor volume, the optic disc and the eye lens when treating tumors of 6.5, 7, and 7.5 mm of apical height placed in an equatorial position. All plaques are centrically placed. According to our criteria, the treatment of tumors with apical height of 7 and 7.5 mm should not be considered since the required dose at the sclera in order to reach 100 Gy at the apex is 1,673 and 1,920 Gy, respectively. Nevertheless, the DVHs of the tumor volume for these large tumors are plotted.

For tumors of 3 mm of apical height in a posterior position, it was found that the CCA1364 eye plaque placed eccentrically and not fully covering the base of the tumor by at most 0.3 mm delivers the most suitable treatment, among those considered, in terms of the studied DVHs. For this tumor height and location, the most conservative treatment with respect to the optic disc is given by the CCB1256 plaque in an equatorial placement although the criterion of 100 Gy at the apex is not achieved.

In Figure 6, the DVHs corresponding to the treatment of equatorial tumors of 3 and 5 mm of apical height are plotted, using for the simulation the dose criterion of 700 Gy at the sclera. For tumors of 3 mm of apical height, the maximum apical dose is 237 Gy, delivered by the CCB1256 plaque. The CCA1364 delivers a 7% smaller dose and the homogeneous CCA and CCB plaques deliver a 34 and 54% lower dose than the CCB1256 plaque, respectively. With respect to the tumor of 5 mm of apical height, the best coverage and maximum dose of 107 Gy at the apex is given by the CCB1256 plaque. The CCA1364 delivers an 18% smaller dose than the CCB1256 plaque, therefore not reaching the required dose of 100 Gy at the tumor apex. For this tumor size, the homogeneous CCA and CCB plaques do not accomplish the treatment criterion of 100 Gy at the tumor apex, while delivering 700 Gy to the sclera.

For tumors with an apical height of less than 5 mm in equatorial position and taking into consideration the criterion of 700 Gy at the sclera, the CCB1256 eye plaque succeeds with a good coverage of the tumor volume. The CCA1364 eye plaque does not succeed for a tumor of 5 mm of apical height since the dose delivered at the apex is 88 Gy.

For tumors of a height larger than 5 mm, the criterion to extend the irradiation time until the dose at the tumor apex reaches 100 Gy must be used. DVHs of the tumor volume, the optic disc, and the eye lens are plotted in Figure 7 for the irradiations considering equatorial tumors of apical heights of 6.5, 7, and 7.5 mm. For tumors of 6.5 mm of apical height, the CCA1364 and the CCB1256 plaques do not exceed the dose of 1,500 Gy at the sclera in order to reach 100 Gy at the apex. The CCB1256 plaque is the most conservative one delivering 1,182 Gy; the CCA1364 delivers a 25% higher dose than the CCB1256 at the sclera. According to the dose prescription presented at the end of section 2, tumors of 7 and 7.5 mm cannot be treated because the maximum dose of 1,500 Gy allowed at the sclera cannot be respected.

Tumors of 6.5 mm of apical height can be treated with the CCA1364 and CCB1256 eye plaques. Both plaques succeed without delivering more than 1,500 Gy at the

sclera. The most conservative treatment with respect to the eye lens and the optic disc is given by the CCA1364 eye plaque. For tumors of an apical height larger than 7 mm all plaques deliver doses at the sclera that exceed the limit considered previously.

Conclusions

The heterogeneous distribution of the activity at the active layer of the applicator has an important contribution to the dose distribution in the irradiated volume and might be used to the benefit of the patient. By taking advantage of the heterogeneous distribution of the emitter map, it is possible to reduce the dose to structures at risk and to increase the applied dose to the tumor volume. In general, the emitter map of every single plaque is not known, hence it must be measured with specific experimental setups that are not part of the routine clinical practice. Currently there is no such system that allows routine measurements of the emitter map and its usage in the subsequent Monte Carlo simulation. Therefore, the heterogeneous activity distribution of the plaque has to be considered as another uncertainty which might become relevant when treating tumors with an apical height larger than 3 mm.

Statement of Ethics

The authors have no ethical conflicts to disclose.

Disclosure Statement

The authors are thankful to the Deutsche Forschungsgemeinschaft (projects BR 4043/3-1, FL 733/1-1, and EI 869/1-3). The authors declare that there does not exist any conflict of interest.

References

1 Astrahan MA. A patch source model for treatment planning of ruthenium ophthalmic applicators. Med Phys. 2003 Jun;30(6):1219–28.
2 Jager MJ, Desjardins L, Kivelä T, Damato B, editors. Current concepts in uveal melanoma. Basel: Karger; 2012.
3 Nag S, Quivey JM, Earle JD, Followill D, Fontanesi J, Finger PT; American Brachytherapy Society. The American Brachytherapy Society recommendations for brachytherapy of uveal melanomas. Int J Radiat Oncol Biol Phys. 2003 Jun;56(2):544–55.
4 Bergman L, Nilsson B, Lundell G, Lundell M, Seregard S. Ruthenium brachytherapy for uveal melanoma, 1979-2003: survival and functional outcomes in the Swedish population. Ophthalmology. 2005 May;112(5):834–40.
5 Simpson ER, Gallie B, Laperrierre N, Beiki-Ardani A, Kivelä T, Raivio V, et al.; ABS – OOTF Committee. The American Brachytherapy Society consensus guidelines for plaque brachytherapy of uveal melanoma and retinoblastoma. Brachytherapy. 2014 Jan-Feb;13(1):1–14.
6 Das IJ, Ding GX, Ahnesjö A. Small fields: nonequilibrium radiation dosimetry. Med Phys. 2008 Jan;35(1):206–15.
7 Brualla L, Palanco-Zamora R, Wittig A, Sempau J, Sauerwein W. Comparison between PENELOPE and electron Monte Carlo simulations of electron fields used in the treatment of conjunctival lymphoma. Phys Med Biol. 2009 Sep;54(18):5469–81.
8 Cross WG, Hokkanen J, Järvinen H, Mourtada F, Sipilä P, Soares CG, et al. Calculation of beta-ray dose distributions from ophthalmic applicators and comparison with measurements in a model eye. Med Phys. 2001 Jul;28(7):1385–96.
9 Sánchez-Reyes A, Tello JI, Guix B, Salvat F. Monte Carlo calculation of the dose distributions of two 106Ru eye applicators. Radiother Oncol. 1998 Nov;49(2):191–6.
10 Brualla L, Sempau J, Sauerwein W. Comment on "Monte Carlo calculation of the dose distributions of two Ru-106 eye applicators" [Radiother Oncol 49 (1998) 191-196]. Radiother Oncol. 2012 Aug;104(2):267–8.
11 Fuss MC, Muñoz A, Oller JC, Blanco F, Williart A, Limão-Vieira P, et al. Energy deposition by a 106Ru/106Rh eye applicator simulated using LEPTS, a low-energy particle track simulation. Appl Radiat Isot. 2011 Sep;69(9):1198–204.
12 Russo A, Laguardia M, Damato B. Eccentric ruthenium plaque radiotherapy of posterior choroidal melanoma. Graefes Arch Clin Exp Ophthalmol. 2012 Oct;250(10):1533–40.
13 Hermida-López M. Calculation of dose distributions for 12 106Ru/106Rh ophthalmic applicator models with the PENELOPE Monte Carlo code. Med Phys. 2013 Oct;40(10):101705.
14 Barbosa NA, da Rosa LA, de Menezes AF, Reis J, Facure A, Braz D. Assessment of ocular beta radiation dose distribution due to 106Ru/106Rh brachytherapy applicators using MCNPX Monte Carlo code. Int J Cancer. 2014;2(3):02038.
15 Brualla L, Sempau J, Zaragoza FJ, Wittig A, Sauerwein W. Accurate estimation of dose distributions inside an eye irradiated with 106Ru plaques. Strahlenther Onkol. 2013 Jan;189(1):68–73.
16 Brualla L, Zaragoza FJ, Sauerwein W. Monte Carlo simulation of the treatment of eye tumors with 106Ru plaques: a study on maximum tumor height and eccentric placement. Ocul Oncol Pathol. 2014 Oct;1(1):2–12.
17 Hermida-López M, Brualla L. Technical Note: monte Carlo study of 106 Ru/106 Rh ophthalmic plaques including the 106 Rh gamma spectrum. Med Phys. 2017 Jun;44(6):2581–5.
18 Stöckel E, Eichmann M, Flühs D, Sommer H, Biewald E, Bornfeld N, et al. Dose Distributions and Treatment Margins in Ocular Brachytherapy with 106Ru Eye Plaques. Ocul Oncol Pathol. 2018;4:122–8.
19 Hermida-López M, Brualla L. Absorbed dose distributions from ophthalmic 106 Ru/106 Rh plaques measured in water with radiochromic film. Med Phys. 2018 Apr;45(4):1699–707.
20 Zaragoza FJ, Eichmann M, Flühs D, Sauerwein W, Brualla L. Flühs, Sauerwein W, Brualla L. Monte Carlo estimation of absorbed dose distributions obtained from heterogeneous 106Ru eye plaques. Ocul Oncol Pathol. 2017 Sep;3(3):204–9.

21 Eichmann M, Flühs D, Spaan B. Development of a high precision dosimetry system for the measurement of surface dose rate distribution for eye applicators. Med Phys. 2009 Oct; 36(10):4634–43.
22 User manual Ru-106 ophthalmic applicators, Rev 12, English. Berlin: Eckert & Ziegler BEBIG; 2016.
23 Salvat F, Fernández-Varea JM, Sempau J. PENELOPE-2008: A code system for Monte Carlo simulation of electron and photon transport. 2009.
24 De Frenne D, Negret A. Nuclear Data Sheets for A = 106. Nucl Data Sheets. 2009;19:943–1002.
25 Sempau J, Acosta E, Baró J, Fernández-Varea JM, Salvat F. An algorithm for Monte Carlo simulation of coupled electron-photon transport. Nucl Instrum Meth B. 1997;132(3):377–90.
26 Sempau J, Badal A, Brualla L. A PENELOPE-based system for the automated Monte Carlo simulation of clinacs and voxelized geometries-application to far-from-axis fields. Med Phys. 2011 Nov;38(11):5887–95.
27 García-Toraño E, Grau Malonda A. EFFY, a new program to compute the counting efficiency of beta particles in liquid scintillators. Comput Phys Commun. 1985;36(3):307–12.
28 Atchison DA, Jones CE, Schmid KL, Pritchard N, Pope JM, Strugnell WE, et al. Eye shape in emmetropia and myopia. Invest Ophthalmol Vis Sci. 2004 Oct;45(10):3380–6.
29 Brualla L, Palanco-Zamora R, Steuhl KP, Bornfeld N, Sauerwein W. Monte Carlo simulations applied to conjunctival lymphoma radiotherapy treatment. Strahlenther Onkol. 2011 Aug;187(8):492–8.
30 Brualla L, Zaragoza FJ, Sempau J, Wittig A, Sauerwein W. Electron irradiation of conjunctival lymphoma – Monte Carlo simulation of the minute dose distribution and technique optimization. Int J Radiat Oncol Biol Phys. 2012 Jul;83(4):1330–7.
31 Goitein M, Miller T. Planning proton therapy of the eye. Med Phys. 1983 May-Jun;10(3): 275–83.
32 Sheen M. Eyeplan user manual v. 3.01 Douglas Cyclotron Laboratory. Clatterbridge; 2001.